

Measurement of the Λ_b lifetime in the exclusive decay $\Lambda_b \rightarrow J/\psi \Lambda$

V.M. Abazov,³⁵ B. Abbott,⁷⁵ M. Abolins,⁶⁵ B.S. Acharya,²⁸ M. Adams,⁵¹ T. Adams,⁴⁹ E. Aguilo,⁵ S.H. Ahn,³⁰ M. Ahsan,⁵⁹ G.D. Alexeev,³⁵ G. Alkhazov,³⁹ A. Alton,^{64,*} G. Alverson,⁶³ G.A. Alves,² M. Anastasoie,³⁴ L.S. Ancu,³⁴ T. Andeen,⁵³ S. Anderson,⁴⁵ B. Andrieu,¹⁶ M.S. Anzels,⁵³ Y. Arnaud,¹³ M. Arov,⁶⁰ M. Arthaud,¹⁷ A. Askew,⁴⁹ B. Åsman,⁴⁰ A.C.S. Assis Jesus,³ O. Atramentov,⁴⁹ C. Autermann,²⁰ C. Avila,⁷ C. Ay,²³ F. Badaud,¹² A. Baden,⁶¹ L. Bagby,⁵² B. Baldin,⁵⁰ D.V. Bandurin,⁵⁹ P. Banerjee,²⁸ S. Banerjee,²⁸ E. Barberis,⁶³ A.-F. Barfuss,¹⁴ P. Bargassa,⁸⁰ P. Baringer,⁵⁸ J. Barreto,² J.F. Bartlett,⁵⁰ U. Bassler,¹⁶ D. Bauer,⁴³ S. Beale,⁵ A. Bean,⁵⁸ M. Begalli,³ M. Begel,⁷¹ C. Belanger-Champagne,⁴⁰ L. Bellantoni,⁵⁰ A. Bellavance,⁵⁰ J.A. Benitez,⁶⁵ S.B. Beri,²⁶ G. Bernardi,¹⁶ R. Bernhard,²² L. Berntzon,¹⁴ I. Bertram,⁴² M. Besançon,¹⁷ R. Beuselinck,⁴³ V.A. Bezzubov,³⁸ P.C. Bhat,⁵⁰ V. Bhatnagar,²⁶ C. Biscarat,¹⁹ G. Blazey,⁵² F. Blekman,⁴³ S. Blessing,⁴⁹ D. Bloch,¹⁸ K. Bloom,⁶⁷ A. Boehnlein,⁵⁰ D. Boline,⁶² T.A. Bolton,⁵⁹ G. Borissoy,⁴² K. Bos,³³ T. Bose,⁷⁷ A. Brandt,⁷⁸ R. Brock,⁶⁵ G. Brooijmans,⁷⁰ A. Bross,⁵⁰ D. Brown,⁷⁸ N.J. Buchanan,⁴⁹ D. Buchholz,⁵³ M. Buehler,⁸¹ V. Buescher,²¹ S. Burdin,^{42,¶} S. Burke,⁴⁵ T.H. Burnett,⁸² C.P. Buszello,⁴³ J.M. Butler,⁶² P. Calfayan,²⁴ S. Calvet,¹⁴ J. Cammin,⁷¹ S. Caron,³³ W. Carvalho,³ B.C.K. Casey,⁷⁷ N.M. Cason,⁵⁵ H. Castilla-Valdez,³² S. Chakrabarti,¹⁷ D. Chakraborty,⁵² K. Chan,⁵ K.M. Chan,⁵⁵ A. Chandra,⁴⁸ F. Charles,¹⁸ E. Cheu,⁴⁵ F. Chevallier,¹³ D.K. Cho,⁶² S. Choi,³¹ B. Choudhary,²⁷ L. Christofek,⁷⁷ T. Christoudias,⁴³ S. Cihangir,⁵⁰ D. Claes,⁶⁷ B. Clément,¹⁸ C. Clément,⁴⁰ Y. Coadou,⁵ M. Cooke,⁸⁰ W.E. Cooper,⁵⁰ M. Corcoran,⁸⁰ F. Couderc,¹⁷ M.-C. Cousinou,¹⁴ S. Crépe-Renaudin,¹³ D. Cutts,⁷⁷ M. Cwiok,²⁹ H. da Motta,² A. Das,⁶² G. Davies,⁴³ K. De,⁷⁸ P. de Jong,³³ S.J. de Jong,³⁴ E. De La Cruz-Burelo,⁶⁴ C. De Oliveira Martins,³ J.D. Degenhardt,⁶⁴ F. Déliot,¹⁷ M. Demarteau,⁵⁰ R. Demina,⁷¹ D. Denisov,⁵⁰ S.P. Denisov,³⁸ S. Desai,⁵⁰ H.T. Diehl,⁵⁰ M. Diesburg,⁵⁰ A. Dominguez,⁶⁷ H. Dong,⁷² L.V. Dudko,³⁷ L. Duflot,¹⁵ S.R. Dugad,²⁸ D. Duggan,⁴⁹ A. Duperrin,¹⁴ J. Dyer,⁶⁵ A. Dyshkant,⁵² M. Eads,⁶⁷ D. Edmunds,⁶⁵ J. Ellison,⁴⁸ V.D. Elvira,⁵⁰ Y. Enari,⁷⁷ S. Eno,⁶¹ P. Ermolov,³⁷ H. Evans,⁵⁴ A. Evdokimov,⁷³ V.N. Evdokimov,³⁸ A.V. Ferapontov,⁵⁹ T. Ferbel,⁷¹ F. Fiedler,²⁴ F. Filthaut,³⁴ W. Fisher,⁵⁰ H.E. Fisk,⁵⁰ M. Ford,⁴⁴ M. Fortner,⁵² H. Fox,²² S. Fu,⁵⁰ S. Fuess,⁵⁰ T. Gadfort,⁸² C.F. Galea,³⁴ E. Gallas,⁵⁰ E. Galyaev,⁵⁵ C. Garcia,⁷¹ A. Garcia-Bellido,⁸² V. Gavrilov,³⁶ P. Gay,¹² W. Geist,¹⁸ D. Gelé,¹⁸ C.E. Gerber,⁵¹ Y. Gershtein,⁴⁹ D. Gillberg,⁵ G. Gintler,⁷¹ N. Gollub,⁴⁰ B. Gómez,⁷ A. Goussiou,⁵⁵ P.D. Grannis,⁷² H. Greenlee,⁵⁰ Z.D. Greenwood,⁶⁰ E.M. Gregores,⁴ G. Grenier,¹⁹ Ph. Gris,¹² J.-F. Grivaz,¹⁵ A. Grohsjean,²⁴ S. Grünendahl,⁵⁰ M.W. Grünewald,²⁹ F. Guo,⁷² J. Guo,⁷² G. Gutierrez,⁵⁰ P. Gutierrez,⁷⁵ A. Haas,⁷⁰ N.J. Hadley,⁶¹ P. Haefner,²⁴ S. Hagopian,⁴⁹ J. Haley,⁶⁸ I. Hall,⁷⁵ R.E. Hall,⁴⁷ L. Han,⁶ K. Hanagaki,⁵⁰ P. Hansson,⁴⁰ K. Harder,⁴⁴ A. Harel,⁷¹ R. Harrington,⁶³ J.M. Hauptman,⁵⁷ R. Hauser,⁶⁵ J. Hays,⁴³ T. Hebbeker,²⁰ D. Hedin,⁵² J.G. Hegeman,³³ J.M. Heinmiller,⁵¹ A.P. Heinson,⁴⁸ U. Heintz,⁶² C. Hensel,⁵⁸ K. Herner,⁷² G. Hesketh,⁶³ M.D. Hildreth,⁵⁵ R. Hirosky,⁸¹ J.D. Hobbs,⁷² B. Hoeneisen,¹¹ H. Hoeth,²⁵ M. Hohlfeld,²¹ S.J. Hong,³⁰ R. Hooper,⁷⁷ S. Hossain,⁷⁵ P. Houben,³³ Y. Hu,⁷² Z. Hubacek,⁹ V. Hynek,⁸ I. Iashvili,⁶⁹ R. Illingworth,⁵⁰ A.S. Ito,⁵⁰ S. Jabeen,⁶² M. Jaffré,¹⁵ S. Jain,⁷⁵ K. Jakobs,²² C. Jarvis,⁶¹ R. Jesik,⁴³ K. Johns,⁴⁵ C. Johnson,⁷⁰ M. Johnson,⁵⁰ A. Jonckheere,⁵⁰ P. Jonsson,⁴³ A. Juste,⁵⁰ D. Käfer,²⁰ S. Kahn,⁷³ E. Kajfasz,¹⁴ A.M. Kalinin,³⁵ J.M. Kalk,⁶⁰ J.R. Kalk,⁶⁵ S. Kappler,²⁰ D. Karmanov,³⁷ J. Kasper,⁶² P. Kasper,⁵⁰ I. Katsanos,⁷⁰ D. Kau,⁴⁹ R. Kaur,²⁶ V. Kaushik,⁷⁸ R. Kehoe,⁷⁹ S. Kermiche,¹⁴ N. Khalatyan,³⁸ A. Khanov,⁷⁶ A. Kharchilava,⁶⁹ Y.M. Khazdheev,³⁵ D. Khatidze,⁷⁰ H. Kim,³¹ T.J. Kim,³⁰ M.H. Kirby,³⁴ M. Kirsch,²⁰ B. Klima,⁵⁰ J.M. Kohli,²⁶ J.-P. Konrath,²² M. Kopal,⁷⁵ V.M. Korablev,³⁸ B. Kothari,⁷⁰ A.V. Kozelov,³⁸ D. Krop,⁵⁴ A. Kryemadhi,⁸¹ T. Kuhl,²³ A. Kumar,⁶⁹ S. Kunori,⁶¹ A. Kupco,¹⁰ T. Kurča,¹⁹ J. Kvita,⁸ D. Lam,⁵⁵ S. Lammers,⁷⁰ G. Landsberg,⁷⁷ J. Lazoflores,⁴⁹ P. Lebrun,¹⁹ W.M. Lee,⁵⁰ A. Leflat,³⁷ F. Lehner,⁴¹ J. Lellouch,¹⁶ V. Lesne,¹² J. Leveque,⁴⁵ P. Lewis,⁴³ J. Li,⁷⁸ L. Li,⁴⁸ Q.Z. Li,⁵⁰ S.M. Lietti,⁴ J.G.R. Lima,⁵² D. Lincoln,⁵⁰ J. Linnemann,⁶⁵ V.V. Lipaev,³⁸ R. Lipton,⁵⁰ Y. Liu,⁶ Z. Liu,⁵ L. Lobo,⁴³ A. Lobodenko,³⁹ M. Lokajicek,¹⁰ A. Lounis,¹⁸ P. Love,⁴² H.J. Lubatti,⁸² A.L. Lyon,⁵⁰ A.K.A. Maciel,² D. Mackin,⁸⁰ R.J. Madaras,⁴⁶ P. Mättig,²⁵ C. Magass,²⁰ A. Magerkurth,⁶⁴ N. Makovec,¹⁵ P.K. Mal,⁵⁵ H.B. Malbouisson,³ S. Malik,⁶⁷ V.L. Malyshev,³⁵ H.S. Mao,⁵⁰ Y. Maravin,⁵⁹ B. Martin,¹³ R. McCarthy,⁷² A. Melnitchouk,⁶⁶ A. Mendes,¹⁴ L. Mendoza,⁷ P.G. Mercadante,⁴ M. Merkin,³⁷ K.W. Merritt,⁵⁰ A. Meyer,²⁰ J. Meyer,²¹ M. Michaut,¹⁷ T. Millet,¹⁹ J. Mitrevski,⁷⁰ J. Molina,³ R.K. Mommsen,⁴⁴ N.K. Mondal,²⁸ R.W. Moore,⁵ T. Moulik,⁵⁸ G.S. Muanza,¹⁹ M. Mulders,⁵⁰ M. Mulhearn,⁷⁰ O. Mundal,²¹ L. Mundim,³ E. Nagy,¹⁴ M. Naimuddin,⁵⁰ M. Narain,⁷⁷ N.A. Naumann,³⁴ H.A. Neal,⁶⁴ J.P. Negret,⁷ P. Neustroev,³⁹ H. Nilsen,²² C. Noeding,²² A. Nomerotski,⁵⁰

S.F. Novaes,⁴ T. Nunnemann,²⁴ V. O'Dell,⁵⁰ D.C. O'Neil,⁵ G. Obrant,³⁹ C. Ochando,¹⁵ D. Onoprienko,⁵⁹ N. Oshima,⁵⁰ J. Osta,⁵⁵ R. Otec,⁹ G.J. Otero y Garzón,⁵¹ M. Owen,⁴⁴ P. Padley,⁸⁰ M. Pangilinan,⁷⁷ N. Panikashvili,^{64,†} N. Parashar,⁵⁶ S.-J. Park,⁷¹ S.K. Park,³⁰ J. Parsons,⁷⁰ R. Partridge,⁷⁷ N. Parua,⁵⁴ A. Patwa,⁷³ G. Pawloski,⁸⁰ P.M. Perea,⁴⁸ K. Peters,⁴⁴ Y. Peters,²⁵ P. Pétrouff,¹⁵ M. Petteni,⁴³ R. Piegai,¹ J. Piper,⁶⁵ M.-A. Pleier,²¹ P.L.M. Podesta-Lerma,^{32,§} V.M. Podstavkov,⁵⁰ Y. Pogorelov,⁵⁵ M.-E. Pol,² A. Pompoš,⁷⁵ B.G. Pope,⁶⁵ A.V. Popov,³⁸ C. Potter,⁵ W.L. Prado da Silva,³ H.B. Prosper,⁴⁹ S. Protopopescu,⁷³ J. Qian,⁶⁴ A. Quadt,²¹ B. Quinn,⁶⁶ A. Rakitine,⁴² M.S. Rangel,² K.J. Rani,²⁸ K. Ranjan,²⁷ P.N. Ratoff,⁴² P. Renkel,⁷⁹ S. Reucroft,⁶³ P. Rich,⁴⁴ M. Rijssenbeek,⁷² I. Ripp-Baudot,¹⁸ F. Rizatdinova,⁷⁶ S. Robinson,⁴³ R.F. Rodrigues,³ C. Royon,¹⁷ P. Rubinov,⁵⁰ R. Ruchti,⁵⁵ G. Safronov,³⁶ G. Sajot,¹³ A. Sánchez-Hernández,³² M.P. Sanders,¹⁶ A. Santoro,³ G. Savage,⁵⁰ L. Sawyer,⁶⁰ T. Scanlon,⁴³ D. Schaile,²⁴ R.D. Schamberger,⁷² Y. Scheglov,³⁹ H. Schellman,⁵³ P. Schieferdecker,²⁴ T. Schliephake,²⁵ C. Schmitt,²⁵ C. Schwanenberger,⁴⁴ A. Schwartzman,⁶⁸ R. Schwienhorst,⁶⁵ J. Sekaric,⁴⁹ S. Sengupta,⁴⁹ H. Severini,⁷⁵ E. Shabalina,⁵¹ M. Shamim,⁵⁹ V. Shary,¹⁷ A.A. Shchukin,³⁸ R.K. Shivpuri,²⁷ D. Shpakov,⁵⁰ V. Siccaldi,¹⁸ V. Simak,⁹ V. Sirotenko,⁵⁰ P. Skubic,⁷⁵ P. Slattery,⁷¹ D. Smirnov,⁵⁵ R.P. Smith,⁵⁰ G.R. Snow,⁶⁷ J. Snow,⁷⁴ S. Snyder,⁷³ S. Söldner-Rembold,⁴⁴ L. Sonnenschein,¹⁶ A. Sopczak,⁴² M. Sosebee,⁷⁸ K. Soustruznik,⁸ M. Souza,² B. Spurlock,⁷⁸ J. Stark,¹³ J. Steele,⁶⁰ V. Stolin,³⁶ A. Stone,⁵¹ D.A. Stoyanova,³⁸ J. Strandberg,⁶⁴ S. Strandberg,⁴⁰ M.A. Strang,⁶⁹ M. Strauss,⁷⁵ R. Ströhmer,²⁴ D. Strom,⁵³ M. Strovink,⁴⁶ L. Stutte,⁵⁰ S. Sumowidagdo,⁴⁹ P. Svoisky,⁵⁵ A. Sznajder,³ M. Talby,¹⁴ P. Tamburello,⁴⁵ A. Tanasijczuk,¹ W. Taylor,⁵ P. Telford,⁴⁴ J. Temple,⁴⁵ B. Tiller,²⁴ F. Tissandier,¹² M. Titov,¹⁷ V.V. Tokmenin,³⁵ M. Tomoto,⁵⁰ T. Toole,⁶¹ I. Torchiani,²² T. Trefzger,²³ D. Tsybychev,⁷² B. Tuchming,¹⁷ C. Tully,⁶⁸ P.M. Tuts,⁷⁰ R. Unalan,⁶⁵ L. Uvarov,³⁹ S. Uvarov,³⁹ S. Uzunyan,⁵² B. Vachon,⁵ P.J. van den Berg,³³ B. van Eijk,³⁵ R. Van Kooten,⁵⁴ W.M. van Leeuwen,³³ N. Varelas,⁵¹ E.W. Varnes,⁴⁵ A. Vartapetian,⁷⁸ I.A. Vasilyev,³⁸ M. Vaupel,²⁵ P. Verdier,¹⁹ L.S. Vertogradov,³⁵ M. Verzocchi,⁵⁰ F. Villeneuve-Segui,⁴³ P. Vint,⁴³ E. Von Toerne,⁵⁹ M. Voutilainen,^{67,‡} M. Vreeswijk,³³ R. Wagner,⁶⁸ H.D. Wahl,⁴⁹ L. Wang,⁶¹ M.H.L.S Wang,⁵⁰ J. Warchol,⁵⁵ G. Watts,⁸² M. Wayne,⁵⁵ G. Weber,²³ M. Weber,⁵⁰ H. Weerts,⁶⁵ A. Wenger,^{22,#} N. Wermes,²¹ M. Wetstein,⁶¹ A. White,⁷⁸ D. Wicke,²⁵ G.W. Wilson,⁵⁸ S.J. Wimpenny,⁴⁸ M. Wobisch,⁶⁰ D.R. Wood,⁶³ T.R. Wyatt,⁴⁴ Y. Xie,⁷⁷ S. Yacoob,⁵³ R. Yamada,⁵⁰ M. Yan,⁶¹ T. Yasuda,⁵⁰ Y.A. Yatsunenko,³⁵ K. Yip,⁷³ H.D. Yoo,⁷⁷ S.W. Youn,⁵³ C. Yu,¹³ J. Yu,⁷⁸ A. Yurkewicz,⁷² A. Zatserklyaniy,⁵² C. Zeitnitz,²⁵ D. Zhang,⁵⁰ T. Zhao,⁸² B. Zhou,⁶⁴ J. Zhu,⁷² M. Zielinski,⁷¹ D. Zieminska,⁵⁴ A. Zieminski,⁵⁴ L. Zivkovic,⁷⁰ V. Zutshi,⁵² and E.G. Zverev³⁷ (DØ Collaboration)

¹ Universidad de Buenos Aires, Buenos Aires, Argentina

² LAFEX, Centro Brasileiro de Pesquisas Físicas, Rio de Janeiro, Brazil

³ Universidade do Estado do Rio de Janeiro, Rio de Janeiro, Brazil

⁴ Instituto de Física Teórica, Universidade Estadual Paulista, São Paulo, Brazil

⁵ University of Alberta, Edmonton, Alberta, Canada, Simon Fraser University, Burnaby, British Columbia, Canada, York University, Toronto, Ontario, Canada, and McGill University, Montreal, Quebec, Canada

⁶ University of Science and Technology of China, Hefei, People's Republic of China

⁷ Universidad de los Andes, Bogotá, Colombia

⁸ Center for Particle Physics, Charles University, Prague, Czech Republic

⁹ Czech Technical University, Prague, Czech Republic

¹⁰ Center for Particle Physics, Institute of Physics, Academy of Sciences of the Czech Republic, Prague, Czech Republic

¹¹ Universidad San Francisco de Quito, Quito, Ecuador

¹² Laboratoire de Physique Corpusculaire, IN2P3-CNRS, Université Blaise Pascal, Clermont-Ferrand, France

¹³ Laboratoire de Physique Subatomique et de Cosmologie, IN2P3-CNRS, Université de Grenoble 1, Grenoble, France

¹⁴ CPPM, IN2P3-CNRS, Université de la Méditerranée, Marseille, France

¹⁵ Laboratoire de l'Accélérateur Linéaire, IN2P3-CNRS et Université Paris-Sud, Orsay, France

¹⁶ LPNHE, IN2P3-CNRS, Universités Paris VI and VII, Paris, France

¹⁷ DAPNIA/Service de Physique des Particules, CEA, Saclay, France

¹⁸ IPHC, Université Louis Pasteur et Université de Haute Alsace, CNRS, IN2P3, Strasbourg, France

¹⁹ IPNL, Université Lyon 1, CNRS/IN2P3, Villeurbanne, France and Université de Lyon, Lyon, France

²⁰ III. Physikalisches Institut A, RWTH Aachen, Aachen, Germany

²¹ Physikalisches Institut, Universität Bonn, Bonn, Germany

²² Physikalisches Institut, Universität Freiburg, Freiburg, Germany

²³ Institut für Physik, Universität Mainz, Mainz, Germany

²⁴ Ludwig-Maximilians-Universität München, München, Germany

²⁵ Fachbereich Physik, University of Wuppertal, Wuppertal, Germany

²⁶ Panjab University, Chandigarh, India

²⁷ Delhi University, Delhi, India

- ²⁸ Tata Institute of Fundamental Research, Mumbai, India
²⁹ University College Dublin, Dublin, Ireland
³⁰ Korea Detector Laboratory, Korea University, Seoul, Korea
³¹ SungKyunKwan University, Suwon, Korea
³² CINVESTAV, Mexico City, Mexico
³³ FOM-Institute NIKHEF and University of Amsterdam/NIKHEF, Amsterdam, The Netherlands
³⁴ Radboud University Nijmegen/NIKHEF, Nijmegen, The Netherlands
³⁵ Joint Institute for Nuclear Research, Dubna, Russia
³⁶ Institute for Theoretical and Experimental Physics, Moscow, Russia
³⁷ Moscow State University, Moscow, Russia
³⁸ Institute for High Energy Physics, Protvino, Russia
³⁹ Petersburg Nuclear Physics Institute, St. Petersburg, Russia
⁴⁰ Lund University, Lund, Sweden, Royal Institute of Technology and Stockholm University, Stockholm, Sweden, and Uppsala University, Uppsala, Sweden
⁴¹ Physik Institut der Universität Zürich, Zürich, Switzerland
⁴² Lancaster University, Lancaster, United Kingdom
⁴³ Imperial College, London, United Kingdom
⁴⁴ University of Manchester, Manchester, United Kingdom
⁴⁵ University of Arizona, Tucson, Arizona 85721, USA
⁴⁶ Lawrence Berkeley National Laboratory and University of California, Berkeley, California 94720, USA
⁴⁷ California State University, Fresno, California 93740, USA
⁴⁸ University of California, Riverside, California 92521, USA
⁴⁹ Florida State University, Tallahassee, Florida 32306, USA
⁵⁰ Fermi National Accelerator Laboratory, Batavia, Illinois 60510, USA
⁵¹ University of Illinois at Chicago, Chicago, Illinois 60607, USA
⁵² Northern Illinois University, DeKalb, Illinois 60115, USA
⁵³ Northwestern University, Evanston, Illinois 60208, USA
⁵⁴ Indiana University, Bloomington, Indiana 47405, USA
⁵⁵ University of Notre Dame, Notre Dame, Indiana 46556, USA
⁵⁶ Purdue University Calumet, Hammond, Indiana 46323, USA
⁵⁷ Iowa State University, Ames, Iowa 50011, USA
⁵⁸ University of Kansas, Lawrence, Kansas 66045, USA
⁵⁹ Kansas State University, Manhattan, Kansas 66506, USA
⁶⁰ Louisiana Tech University, Ruston, Louisiana 71272, USA
⁶¹ University of Maryland, College Park, Maryland 20742, USA
⁶² Boston University, Boston, Massachusetts 02215, USA
⁶³ Northeastern University, Boston, Massachusetts 02115, USA
⁶⁴ University of Michigan, Ann Arbor, Michigan 48109, USA
⁶⁵ Michigan State University, East Lansing, Michigan 48824, USA
⁶⁶ University of Mississippi, University, Mississippi 38677, USA
⁶⁷ University of Nebraska, Lincoln, Nebraska 68588, USA
⁶⁸ Princeton University, Princeton, New Jersey 08544, USA
⁶⁹ State University of New York, Buffalo, New York 14260, USA
⁷⁰ Columbia University, New York, New York 10027, USA
⁷¹ University of Rochester, Rochester, New York 14627, USA
⁷² State University of New York, Stony Brook, New York 11794, USA
⁷³ Brookhaven National Laboratory, Upton, New York 11973, USA
⁷⁴ Langston University, Langston, Oklahoma 73050, USA
⁷⁵ University of Oklahoma, Norman, Oklahoma 73019, USA
⁷⁶ Oklahoma State University, Stillwater, Oklahoma 74078, USA
⁷⁷ Brown University, Providence, Rhode Island 02912, USA
⁷⁸ University of Texas, Arlington, Texas 76019, USA
⁷⁹ Southern Methodist University, Dallas, Texas 75275, USA
⁸⁰ Rice University, Houston, Texas 77005, USA
⁸¹ University of Virginia, Charlottesville, Virginia 22901, USA
⁸² University of Washington, Seattle, Washington 98195, USA

(Dated: April 30, 2007)

We have measured the Λ_b lifetime using the exclusive decay $\Lambda_b \rightarrow J/\psi \Lambda$, based on 1.2 fb^{-1} of data collected with the D0 detector during 2002–2006. From 171 reconstructed Λ_b decays, where the J/ψ and Λ are identified via the decays $J/\psi \rightarrow \mu^+ \mu^-$ and $\Lambda \rightarrow p\pi$, we measured the Λ_b lifetime to be $\tau(\Lambda_b) = 1.218^{+0.130}_{-0.115}(\text{stat}) \pm 0.042(\text{syst})$ ps. We also measured the B^0 lifetime in the decay $B^0 \rightarrow J/\psi(\mu^+ \mu^-) K_S^0(\pi^+ \pi^-)$ to be $\tau(B^0) = 1.501^{+0.078}_{-0.074}(\text{stat}) \pm 0.050(\text{syst})$ ps, yielding a lifetime

ratio of $\tau(\Lambda_b)/\tau(B^0) = 0.811_{-0.087}^{+0.096}(\text{stat}) \pm 0.034(\text{syst})$. These measurements are consistent with the current world averages and support the shorter lifetime of the Λ_b with respect to B mesons, in contrast to another recent measurement of significant precision [8].

PACS numbers: 14.20.Mr, 14.40.Nd, 13.30.Eg, 13.25.Hw

Lifetime measurements of b hadrons provide important information on the interactions between heavy and light quarks. At leading order in Heavy Quark Effective Theory (HQET) [1], light quarks are considered spectators and all b hadrons have the same lifetime. Differences arise at higher orders when corrections from interactions are taken into account. For HQET calculations of order $1/m_b^2$, where m_b is the mass of the b quark, the agreement between the predicted lifetimes and the experimental results is excellent for B mesons [2]. However, in the b baryon sector, the world average of measurements of $\tau(\Lambda_b)/\tau(B^0) = 0.844 \pm 0.043$ [3] is smaller than the prediction of the ratio at this order. Recently there have been significant improvements in theoretical calculations of $\tau(\Lambda_b)/\tau(B^0)$. Next-to-leading order effects in QCD [4], corrections at $\mathcal{O}(1/m_b^4)$ in HQET [5], and lattice QCD studies [6], have led to an improved theoretical prediction, $\tau(\Lambda_b)/\tau(B^0) = 0.88 \pm 0.05$ [7]. This value agrees with previous experiments to within the current theoretical and experimental uncertainties. However, a recent measurement [8] reports a value of the Λ_b lifetime consistent with B meson lifetimes, and the ratio $\tau(\Lambda_b)/\tau(B^0)$ consistent with unity. Additional precise measurements of the Λ_b lifetime and $\tau(\Lambda_b)/\tau(B^0)$ ratio may help settle this question.

In this Letter, we report measurements of the Λ_b lifetime using the exclusive decay $\Lambda_b \rightarrow J/\psi + \Lambda$, and its ratio to the B^0 lifetime using the $B^0 \rightarrow J/\psi + K_S^0$ decay channel. This B^0 decay channel is chosen because of its similar topology to the Λ_b decay. The J/ψ is reconstructed from the $\mu^+\mu^-$ decay mode, the Λ from $p\pi^-$, and the K_S^0 from $\pi^+\pi^-$. Throughout this Letter, the appearance of a specific charge state also implies its charge conjugate. The data used in this analysis were collected during 2002–2006 with the D0 detector in Run II of the Tevatron Collider at a center-of-mass energy of 1.96 TeV, and correspond to an integrated luminosity of 1.2 fb^{-1} .

The D0 detector is described in detail elsewhere [9]. The detector components most relevant to this analysis are the central tracking and the muon systems. The former consists of a silicon microstrip tracker (SMT) and a central scintillating fiber tracker (CFT) surrounded by a 2 T superconducting solenoidal magnet. The SMT has a design optimized for tracking and vertexing for pseudorapidity of $|\eta| < 3$ [10]. For charged particles, the resolution on the distance of closest approach as provided by the tracking system is approximately $50 \mu\text{m}$ for tracks with $p_T \approx 1 \text{ GeV}/c$, where p_T is the component of the momentum perpendicular to the beam axis. It improves asymptotically to $15 \mu\text{m}$ for tracks with $p_T > 10 \text{ GeV}/c$.

Preshower detectors and electromagnetic and hadronic calorimeters surround the tracker. The muon system is located beyond the calorimeter, and consists of multilayer drift chambers and scintillation counters inside 1.8 T toroidal magnets, and two similar layers outside the toroids. Muon identification for $|\eta| < 1$ relies on 10 cm wide drift tubes, while 1 cm mini-drift tubes are used for $1 < |\eta| < 2$.

The primary vertex of the $p\bar{p}$ interaction is determined for each event using the average position of the beam-collision in the plane perpendicular to the beam as a constraint. The precision of the primary vertex reconstruction is on average $20 \mu\text{m}$ in the plane perpendicular to the beam and about $40 \mu\text{m}$ along the direction of the beam.

We base our data selection on reconstructed charged tracks and identified muons. Although we do not require any specific trigger, most of the selected events satisfy dimuon or muon triggers. To avoid a trigger bias in the lifetime measurement, we reject events that depend on impact parameter based triggers. We start the Λ_b and B^0 reconstruction by searching for events with J/ψ mesons. We then search in these events for Λ and K_S^0 particles. To reconstruct $J/\psi \rightarrow \mu^+\mu^-$ candidates, we select events with at least two muons of opposite charge reconstructed in the tracker and the muon system. The track of each muon candidate must either match hits in the muon system, or have calorimeter energies consistent with a minimum-ionizing particle along the direction of hits extrapolated from the tracking layers. For at least one of the muons, we require hits in all three layers of the muon detector. Both muons are required to have $p_T > 2.5 \text{ GeV}/c$ if they are in the region $|\eta| < 1$. The muon tracks are constrained to originate from a common vertex with a χ^2 probability greater than 1%, and each J/ψ candidate is required to have a mass in the range $2.80\text{--}3.35 \text{ GeV}/c^2$. The $\Lambda \rightarrow p\pi^-$ decays are reconstructed from two tracks of opposite charge constrained to a common vertex with a χ^2 probability greater than 1%. Each Λ candidate is required to have a mass in the range $1.100\text{--}1.128 \text{ GeV}/c^2$. The proton mass is assigned to the track of higher p_T , as observed in Monte Carlo studies. To suppress contamination from cascade decays of more massive baryons such as $\Sigma^0 \rightarrow \Lambda\gamma$ or $\Xi^0 \rightarrow \Lambda\pi^0$, we require the cosine of the angle between the \mathbf{p}_T vector of the Λ and the vector from the J/ψ vertex to the Λ decay vertex to be larger than 0.9999. For Λ 's that decay from Λ_b the cosine of this angle is very close to one. The $K_S^0 \rightarrow \pi^+\pi^-$ selection follows the same criteria, except that for the K_S^0 , the mass window is $0.460\text{--}0.525 \text{ GeV}/c^2$,

and pion mass assignments are used.

We reconstruct the Λ_b and B^0 by performing a constrained fit to a common vertex for either the Λ or K_S^0 and the two muon tracks, with the latter constrained to the J/ψ mass of $3.097 \text{ GeV}/c^2$ [3]. Because of their long decay lengths, a significant fraction of Λ and K_S^0 particles will decay outside the SMT. There is therefore no requirement of SMT hits on the tracks from Λ and K_S^0 decays. To reconstruct the Λ_b (B^0), we first find the Λ (K_S^0) decay vertex, and then extrapolate the momentum vector of the ensuing particle and form a vertex together with the two muon tracks belonging to the J/ψ . If more than one candidate is found in the event, the candidate with the best χ^2 probability is selected as the Λ_b (B^0) candidate. The mass is required to be within the range $5.1\text{--}6.1 \text{ GeV}/c^2$ for Λ_b candidates and within $4.9\text{--}5.7 \text{ GeV}/c^2$ for B^0 candidates. For the choice of the final selection criteria, we optimize $S/\sqrt{S+B}$, where S and B are the number of signal (Λ_b) and background candidates, respectively, by using Monte Carlo estimates for S and data for B . For the Monte Carlo, we use PYTHIA [11] and EVTGEN [12] to produce and decay particles, respectively, and GEANT3 [13] to simulate detector effects. As a result of this optimization, the p_T of the Λ (K_S^0) is required to be greater than 2.4 (1.8) GeV/c , and the total momentum for both Λ_b and B^0 is required to be greater than $5 \text{ GeV}/c$. Finally, any candidate which has been identified as a Λ_b is removed from the B^0 sample.

We determine the decay time of a Λ_b or B^0 by measuring the distance traveled by the b hadron candidate in a plane transverse to the beam direction, and then applying a correction for the Lorentz boost. We define the transverse decay length as $L_{xy} = \mathbf{L}_{xy} \cdot \mathbf{p}_T / p_T$ where \mathbf{L}_{xy} is the vector that points from the primary vertex to the b hadron decay vertex and \mathbf{p}_T is the transverse momentum vector of the b hadron. The event-by-event value of the proper transverse decay length, λ , for the b hadron candidate is given by:

$$\lambda = \frac{L_{xy}}{(\beta\gamma)_T^B} = L_{xy} \frac{cM_B}{p_T}, \quad (1)$$

where $(\beta\gamma)_T^B$ and M_B are the transverse boost and the mass of the b hadron. In our measurement, the value of M_B in Eq. 1 is set to the Particle Data Group (PDG) mass value of Λ_b or B^0 [3]. We require the uncertainty on λ to be less than $500 \mu\text{m}$.

We perform a simultaneous unbinned maximum likelihood fit to the mass and proper decay length distributions. The likelihood function \mathcal{L} is defined by:

$$\mathcal{L} = \frac{(n_s+n_b)^N}{N!} \exp(-n_s - n_b) \times \prod_{j=1}^N \left[\frac{n_s}{n_s+n_b} \mathcal{F}_{\text{sig}}^j + \frac{n_b}{n_s+n_b} \mathcal{F}_{\text{bkg}}^j \right], \quad (2)$$

where n_s and n_b are the expected number of signal and background events in the sample, respectively. N is the

total number of events. $\mathcal{F}_{\text{sig}}^j$ ($\mathcal{F}_{\text{bkg}}^j$) is the product of three probability density functions that model the mass, proper decay length, and uncertainty on proper decay length distributions for the signal (background). We divide the background into two categories, prompt and non-prompt. The prompt background is primarily due to direct production of J/ψ 's which are then randomly combined with a Λ or K_S^0 candidate in the event. The non-prompt background is mainly produced by the combination of J/ψ mesons from b hadron decays with Λ or K_S^0 candidates present in the event.

For the signal, the mass distribution is modeled by a Gaussian function, and the λ distribution is parametrized by an exponential decay convoluted with the resolution function:

$$G(\lambda_j, \sigma_j) = \frac{1}{\sqrt{2\pi}s\sigma_j} \exp\left[\frac{-\lambda_j^2}{2(s\sigma_j)^2}\right], \quad (3)$$

where λ_j and σ_j represent λ and its uncertainty, respectively, for a given decay j , and s is a common scale parameter introduced in the fit to account for a possible mis-estimate of σ_j . The convolution is defined by:

$$S_\lambda(\lambda_j, \sigma_j) = \frac{1}{\lambda_B} \int_0^\infty G(x - \lambda_j, \sigma_j) \exp\left(\frac{-x}{\lambda_B}\right) dx, \quad (4)$$

where $\lambda_B = c\tau_B$, and τ_B is the lifetime of the Λ_b (B^0). The distribution of the uncertainty of λ is modeled by an exponential function convoluted by a Gaussian.

For the background, the mass distribution of the prompt component is assumed to follow a flat distribution as observed in data when a cut of $\lambda > 100 \mu\text{m}$ is applied. The non-prompt component is modeled with a second-order polynomial function. The λ distribution is parametrized by the resolution function for the prompt component, and by the sum of negative and positive exponential functions for the non-prompt component. A positive and a negative exponential functions model combinatorial background, and an exponential function accounts for long-lived heavy flavor decays. The distribution of the uncertainty of λ is modeled by two exponential functions convoluted by a Gaussian.

We minimize $-2 \ln \mathcal{L}$ to extract: $c\tau(\Lambda_b) = 365.1_{-34.7}^{+39.1} \mu\text{m}$ and $c\tau(B^0) = 450.0_{-22.1}^{+23.5} \mu\text{m}$. From the fits, we obtain $s = 1.41 \pm 0.05$ for the Λ_b and $s = 1.41 \pm 0.03$ for the B^0 . The numbers of signal decays are $171 \pm 20 \Lambda_b$ and $717 \pm 38 B^0$. Figures 1 and 2 show the mass and λ distributions for the Λ_b and B^0 candidates. Fit results are superimposed. Table I summarizes the systematic uncertainties in our measurements. The contribution from possible misalignment of the SMT detector was estimate to be $5.4 \mu\text{m}$ [14]. We estimate the systematic uncertainty due to the models for the λ and mass distributions by varying the parametrizations of the different components: (i) the resolution function is modeled by two Gaussian functions instead of one, (ii)

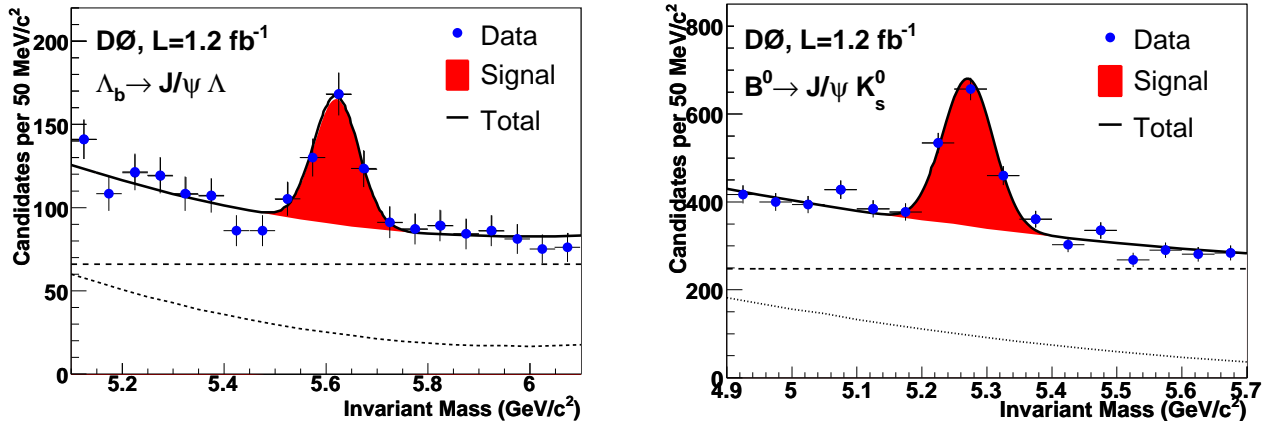


FIG. 1: Invariant mass distribution for Λ_b (left) and B^0 (right) candidates, with the fit results superimposed. The dashed line represents the prompt background component and the dotted line the non-prompt background component. The shaded region represents the signal.

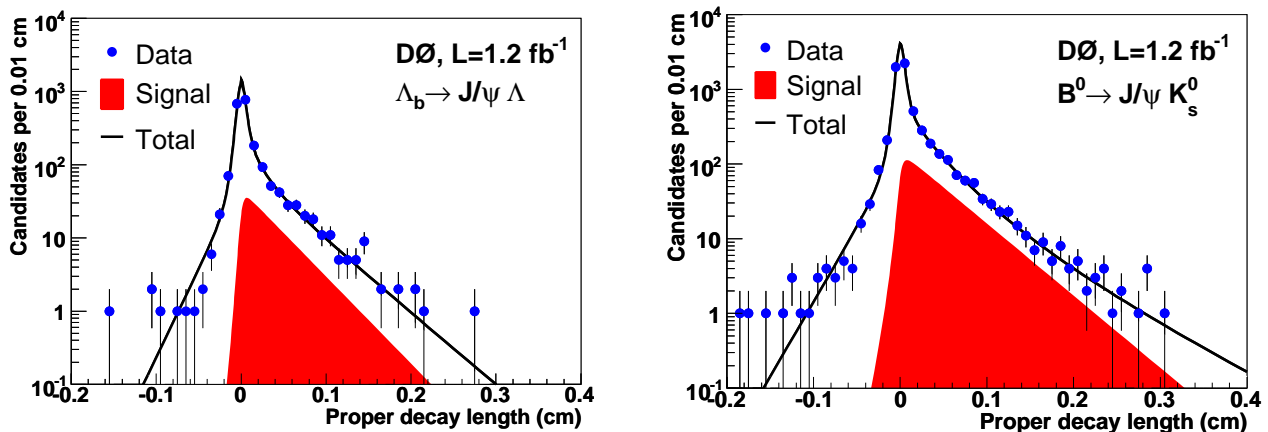


FIG. 2: Proper decay length distribution for Λ_b (left) and B^0 (right) candidates, with the fit results superimposed. The shaded region represents the signal.

the exponential functions in the non-prompt background are replaced by exponentials convoluted with the resolution function, (iii) a uniform background is added to account for outlier events (this has only a negligible effect), (iv) the positive and negative exponentials describing combinatorial non-prompt background are assumed to be symmetric, and (v) for the mass distribution of the non-prompt background, a linear function is used instead of the nominal quadratic form. To take into account correlations between the effects of the different models, a fit that combines all different model changes is performed. We quote the difference between the result of this fit and the nominal fit as the systematic uncertainty.

The lifetime of the background events under the Λ_b (B^0) signal is mostly modeled by events in the low and high mass sideband regions with respect to the peak. To estimate the effect of any difference between the life-

time distributions of these two regions, we perform separate fits to the Λ_b (B^0) mass regions of 5.1–5.8 and 5.4–6.1 GeV/c^2 (4.9–5.45 and 5.1–5.7 GeV/c^2) where the contributions from high and low mass background events are reduced, respectively. The largest difference between these fits and the nominal fit is quoted as the systematic uncertainty due to this source.

We also study the contamination of the Λ_b sample by B^0 events that pass the Λ_b selection. From Monte Carlo studies, we estimate that 6.5% of B^0 events pass the Λ_b selection criteria. However, the invariant mass of B^0 events which contaminate the Λ_b sample is distributed almost uniformly across the entire Λ_b mass range, and their proper decay lengths therefore tend to be incorporated in the long-lived component of the background. To estimate the effect due to this contamination, we remove from the Λ_b sample any event which also passes the B^0

TABLE I: Summary of systematic uncertainties in the measurement of $c\tau$ for Λ_b and B^0 and their ratio. The total uncertainties are determined by combining individual uncertainties in quadrature.

Source	Λ_b (μm)	B^0 (μm)	Ratio
Alignment	5.4	5.4	0.002
Distribution models	6.6	2.8	0.020
Long-lived components	6.0	13.6	0.022
Contamination	7.2	–	0.016
Total	12.7	14.9	0.034

selection criteria, and we perform a fit to the remaining events. The difference between this and the nominal fit is quoted as the systematic uncertainty due to the contamination. For the B^0 , we do not consider this source of systematic uncertainty since any event identified as Λ_b is removed from the B^0 sample.

We perform several cross-checks of the lifetime measurements. The J/ψ vertex is used instead of the b hadron vertex, the mass windows are varied, the reconstructed b hadron mass is used instead of the PDG [3] value, and the sample is split into different pseudorapidity regions and different regions of azimuth. All results obtained with these variations are consistent with our measurement. We also cross-check the fitting procedure and selection criteria by measuring the Λ_b lifetime in Monte Carlo events. The lifetime obtained was consistent with the input value.

The results of our measurement of the Λ_b and B^0 lifetimes are summarized as:

$$c\tau(\Lambda_b) = 365.1_{-34.7}^{+39.1} \text{ (stat)} \pm 12.7 \text{ (syst)} \mu\text{m}, \quad (5)$$

$$c\tau(B^0) = 450.0_{-22.1}^{+23.5} \text{ (stat)} \pm 14.9 \text{ (syst)} \mu\text{m},$$

from which we have:

$$\tau(\Lambda_b) = 1.218_{-0.115}^{+0.130} \text{ (stat)} \pm 0.042 \text{ (syst)} \text{ ps}, \quad (6)$$

$$\tau(B^0) = 1.501_{-0.074}^{+0.078} \text{ (stat)} \pm 0.050 \text{ (syst)} \text{ ps}.$$

These can be combined to determine the ratio of lifetimes:

$$\frac{\tau(\Lambda_b)}{\tau(B^0)} = 0.811_{-0.087}^{+0.096} \text{ (stat)} \pm 0.034 \text{ (syst)}, \quad (7)$$

where we determine the systematic uncertainty on the ratio by calculating the ratio for each systematic source and quoting the deviation in the ratio as the systematic uncertainty due to that source. We combine all systematics in quadrature as shown in Table I. The main contribution to the systematic uncertainty of the lifetime ratio is due to the long-lived component of the B^0 sample. This is expected since the B^0 is more likely than the Λ_b to be contaminated by mis-reconstructed B mesons due to

its lower mass. The ratio of lifetimes, using the world average B^0 lifetime $\tau(B^0) = 1.527 \pm 0.008$ ps [3], is

$$\frac{\tau(\Lambda_b)}{\tau(B^0)} = 0.797_{-0.080}^{+0.089}. \quad (8)$$

In conclusion, we have measured the Λ_b lifetime in the fully reconstructed exclusive decay channel $J/\psi\Lambda$. The measurement is consistent with the world average [3], and the ratio of Λ_b to B^0 lifetimes is consistent with the most recent theoretical predictions [7].

We thank the staffs at Fermilab and collaborating institutions, and acknowledge support from the DOE and NSF (USA); CEA and CNRS/IN2P3 (France); FASI, Rosatom and RFBR (Russia); CAPES, CNPq, FAPERJ, FAPESP and FUNDUNESP (Brazil); DAE and DST (India); Colciencias (Colombia); CONACyT (Mexico); KRF and KOSEF (Korea); CONICET and UBACyT (Argentina); FOM (The Netherlands); Science and Technology Facilities Council (United Kingdom); MSMT and GACR (Czech Republic); CRC Program, CFI, NSERC and WestGrid Project (Canada); BMBF and DFG (Germany); SFI (Ireland); The Swedish Research Council (Sweden); CAS and CNSF (China); Alexander von Humboldt Foundation; and the Marie Curie Program.

-
- [*] Visitor from Augustana College, Sioux Falls, SD, USA.
[¶] Visitor from The University of Liverpool, Liverpool, UK.
[§] Visitor from ICN-UNAM, Mexico City, Mexico.
[‡] Visitor from Helsinki Institute of Physics, Helsinki, Finland.
[†] Visitor from Technion – Israel Institute of Technology, Haifa, Israel.
[#] Visitor from Universität Zürich, Zürich, Switzerland.
- [1] I.I.Y. Bigi *et al.*, Phys. Lett. B **293**, 430 (1992).
[2] M. Neubert and C.T. Sachrajda, Nucl. Phys. B **483**, 339 (1997).
[3] W. M. Yao *et al.*, J. Phys. G **33**, 1 (2006).
[4] E. Franco *et al.*, Nucl. Phys. B **633**, 212 (2002).
[5] F. Gabbiani *et al.*, Phys. Rev. D **68**, 114006 (2003).
[6] M. Di Piero *et al.*, Phys. Lett. B **468**, 143 (1999).
[7] C. Tarantino, Nucl. Phys. B **156**, (Proc. Suppl.), 33 (2006).
[8] A. Abulencia *et al.*, Phys. Rev. Lett. **98**, 122001 (2007).
[9] V. Abazov *et al.*, Nucl. Instrum. Methods A **565**, 463 (2006).
[10] $\eta = -\ln[\tan(\theta/2)]$, where θ is the polar angle with respect to the beamline.
[11] T.Sjöstrand *et al.*, Comp. Phys. Commun. **135**, 238 (2001).
[12] D.J. Lange, Nucl. Instrum. Methods A **462**, 152 (2001).
[13] R. Brun and F. Carminati, CERN Program Library Long Writeup No. W5013, 1993 (unpublished).
[14] V. Abazov *et al.*, Phys. Rev. Lett. **94**, 102001 (2005).